Wigner distribution function of volume holograms

Citation: S. Oh and G. Barbastathis, "Wigner distribution function of volume holograms," Opt. Lett. 34, 2584-2586 (2009).

As Published: http://dx.doi.org/10.1364/OL.34.002584

Publisher: Optical Society of America

Persistent URL: http://hdl.handle.net/1721.1/49444

Version: Author's final manuscript: final author's manuscript post peer review, without publisher's formatting or copy editing

The Wigner distribution function of volume holograms

Se Baek Oh[1,*] and George Barbastathis[1,2]

[1] *Department of Mechanical Engineering, Massachusetts Institute of Technology, 77 Massachusetts Avenue, Cambridge, MA 02139, USA.*

[2] *Singapore–MIT Alliance for Research and Technology (SMART) Centre, Massachusetts Institute of Technology, S16–06–17, 3 Science Drive 2, Singapore 117543*

[*] *Corresponding author: sboh@mit.edu*

Based on a linear systems approach, we derive the Wigner distribution function (WDF) of a 4–f imager with a volume holographic 3D pupil; then we obtain the WDF of the volume hologram itself by using the shearing properties of the WDF. Two common configurations, plane and spherical wave reference volume holograms, are examined in detail. The WDF elucidates the shift variant nature of the volume holographic element in both cases.

OCIS codes: (350.6980) Transforms, (090.7330) Volume gratings, (080.5084) Phase space methods of analysis.

1. Introduction

The Wigner distribution function (WDF) was originally introduced in quantum mechanics [1]. It has also been extremely useful in optics for simultaneously describing the space and spatial–frequency content of optical signals [2]. The WDF of a scalar optical field $g(x)$ is defined as

$$\mathcal{W}_g(x,u) = \int g\left(x+\frac{\xi}{2}\right) g^*\left(x-\frac{\xi}{2}\right) \mathrm{e}^{-i2\pi u\xi} \mathrm{d}\xi, \tag{1}$$

where x denotes the spatial coordinate and u is the local spatial frequency [3]. The WDFs of several thin elements, such as lenses, phase masks, apertures, gratings, etc., have been derived in straightforward fashion by applying eq. (1) to transparencies [4–6]. The WDF typically leads to simple geometrical representations, which provide better intuitive understanding of optical transforms. Since the Bragg selectivity property of volume holograms can have both strong spatial and angular dependence, the WDF is even more appealing for the analysis of volume holographic optical systems such as 3D pupils. However, to our knowledge, the WDF of a 3D pupil has not been derived to date. One reason may be that volume holograms are *not* thin elements; hence, straightforward application of eq. (1) is not feasible.

In this Letter, we show how to derive the WDF of volume holograms (VHs) with arbitrary index modulation and examine two specific examples: plane and spherical wave reference VHs. For notational simplicity, we consider 1–dimensional geometries only, but extension to 2–dimensional geometries is straightforward.

2. WDF of volume holograms

We start from a linear–optical field transformation

$$E_2(x_2) = \int h(x_2; x_1) E_1(x_1) \mathrm{d}x_1, \tag{2}$$

where $h(x_2; x_1)$ denotes a response at the output plane (x_2) produced by an impulse at the input plane (x_1), and E_1 and E_2 are the input and output fields, respectively. Applying the WDF definition to eq. (2), we obtain the input–output relation in Wigner space as

$$\mathcal{W}_2(x_2, u_2) = \iint K_h(x_2, u_2; x_1, u_1) \mathcal{W}_1(x_1, u_1) \mathrm{d}x_1 \mathrm{d}u_1, \tag{3}$$

where

$$K_h(x_2, u_2; x_1, u_1) = \iint h\left(x_2 + \tfrac{x_2'}{2}; x_1 + \tfrac{x_1'}{2}\right) h^*\left(x_2 - \tfrac{x_2'}{2}; x_1 - \tfrac{x_1'}{2}\right) \times \mathrm{e}^{-i2\pi\left(u_2 x_2' - u_1 x_1'\right)} \mathrm{d}x_2' \mathrm{d}x_1'. \tag{4}$$

K_h is the double WDF of the impulse response [7] and represents the system in Wigner space. Since the impulse response of a VH is too complicated to be used in eq. (4), we rather consider the impulse response of a 4–f VH imager, whose geometry is shown in Fig. 1. This is convenient because general forms of its impulse response have been reported previously with the 3D pupil formulation [8]. Assuming Born's first order approximation [9], the impulse response of the 4–f VH imager in the paraxial region is given by

$$h_{4f\mathrm{VH}}(x_2; x_1) = \mathcal{E}\left[\frac{x_1 + x_2}{\lambda f}, \frac{x_1^2 - x_2^2}{2\lambda f^2}\right], \tag{5}$$

where λ is the wavelength, $\mathcal{E}$ is the 2D Fourier transform of a refractive index modulation $\epsilon(x'', z'')$ of the VH [8], and f is the common focal length in the unit magnification 4–f system. Substituting eq. (5) into eqs. (3) and (4), we obtain the Wigner representation of the 4–f VH imager as

$$\mathcal{W}_2(x_2, u_2) = \iint K_{4f\mathrm{VH}}(x_2, u_2; x_1, u_1)\mathcal{W}_1(x_1, u_1)\mathrm{d}x_1\mathrm{d}u_1, \tag{6}$$

where

$$\begin{aligned} K_{4f\mathrm{VH}}(x_2, u_2; x_1, u_1) = \iiiint \mathrm{d}x_1'\mathrm{d}x_2'\mathrm{e}^{-i2\pi\left(u_2x_2' - u_1x_1'\right)} \\ \times \mathcal{E}\left[\frac{x_1 + \frac{x_1'}{2} + x_2 + \frac{x_2'}{2}}{\lambda f}, \frac{(x_1 + \frac{x_1'}{2})^2 - (x_2 + \frac{x_2'}{2})^2}{2\lambda f^2}\right] \\ \times \mathcal{E}^*\left[\frac{x_1 - \frac{x_1'}{2} + x_2 - \frac{x_2'}{2}}{\lambda f}, \frac{(x_1 - \frac{x_1'}{2})^2 - (x_2 - \frac{x_2'}{2})^2}{2\lambda f^2}\right]. \end{aligned} \tag{7}$$

Next we compute the WDF of VHs from eq. (7). As shown in Fig. 1, the input and output WDF to the VH are denoted by $\mathcal{W}_3(x_3, u_3)$ and $\mathcal{W}_4(x_4, u_4)$. They are related to $\mathcal{W}_1$ and $\mathcal{W}_2$ as

$$\mathcal{W}_3(x_3, u_3) = \mathcal{W}_1\left(-\lambda f_1 u_3, \frac{L}{2f}u_3 + \frac{x_3}{\lambda f}\right) \text{ and} \tag{8}$$

$$\mathcal{W}_4(x_4, u_4) = \mathcal{W}_2\left(\lambda f_2 u_4, \frac{L}{2f}u_4 - \frac{x_4}{\lambda f}\right). \tag{9}$$

These relations originate from the well–known properties of the WDF: free–space propagation and phase modulation by a lens produce x– and u–shear in Wigner space, respectively [3]. Using the coordinate transforms in eqs. (8) and (9), we obtain the Wigner representation of a VH as

$$\mathcal{W}_4\left(x_4, u_4\right) = \iint K_{\mathrm{VH}}(x_4, u_4; x_3, u_3)\mathcal{W}_3\left(x_3, u_3\right)\mathrm{d}x_3\mathrm{d}u_3, \tag{10}$$

where

$$K_{\mathrm{VH}}(x_4, u_4; x_3, u_3) = K_{4f\mathrm{VH}}\left(\lambda f u_4, -\frac{L}{2f}u_4 - \frac{x_4}{\lambda f}; -\lambda f u_3, \frac{L}{2f}u_3 + \frac{x_3}{\lambda f}\right). \tag{11}$$

Equation (10) implies that the output WDF, in other words the WDF of the Bragg diffracted field, is computed by the integration of K_{VH} multiplied by the input WDF. Hence, $K_{\mathrm{VH}}(x_4, u_4; x_3, u_3)$ represents the contribution of the input WDF at x_3 and u_3 to the Bragg diffraction originating from x_4 along u_4 direction. In the next section we will show how Bragg selectivity is evidenced in Wigner space.

3. Examples

We examine two common VHs [10, 11] in detail. For simplicity, the lateral dimension of VHs is assumed to be infinitely extended.

3.A. Plane wave reference volume hologram (PRVH)

A PRVH is recorded by two mutually coherent plane waves as shown in Fig. 2(a). The refractive index modulation is

$$\epsilon(x'', z'') = \exp\left\{i\frac{2\pi}{\lambda}\left(\theta_{\mathrm{s}}x'' - \frac{\theta_{\mathrm{s}}^2}{2}z''\right)\right\}\mathrm{rect}\left(\frac{z''}{L}\right), \tag{12}$$

where x'' and z'' are the Cartesian coordinates inside the VH (see Fig. 1). The impulse response of the 4–f VH imager is

$$h(x_2; x_1) = \delta\left(x_1 + x_2 - f\theta_s\right)\mathrm{sinc}\left\{\frac{L}{2\lambda f^2}\left(x_1^2 - x_2^2 + f^2\theta_s^2\right)\right\}. \tag{13}$$

After a long but straightforward derivation [12], an analytical expression of K_{VH} is obtained as

$$K_{\mathrm{VH}}(x_4,u_4;x_3,u_3)=\left(\frac{2}{L\theta_{\mathrm{s}}}\right)\delta\left(u_4-u_3-\frac{\theta_{\mathrm{s}}}{\lambda}\right)\Lambda\left\{\frac{2}{L\theta_{\mathrm{s}}}(x_3-x_4)+\frac{\lambda}{\theta_{\mathrm{s}}}(u_3+u_4)\right\}$$
$$\times\,\mathrm{sinc}\left\{2u_3\left[L\theta_{\mathrm{s}}-\left|L\lambda(u_3+u_4)+2(x_3-x_4)\right|\right]\right\},\quad(14)$$

where Λ denotes the triangle function [13]. Finally, the WDF of the output field is related to the WDF of the input field as

$$\mathcal{W}_4(x_4,u_4)=\left(\frac{2}{L\theta_{\mathrm{s}}}\right)\int\Lambda\left(\frac{L\lambda\left(u_3+\frac{\theta_{\mathrm{s}}}{2\lambda}\right)+(x_3-x_4)}{L\theta_{\mathrm{s}}}\right)$$
$$\times\,\mathrm{sinc}\left\{2u_3\left[L\theta_{\mathrm{s}}-\left|L\theta_{\mathrm{s}}(2u_3+\tfrac{\theta_{\mathrm{s}}}{\lambda})+2(x_3-x_4)\right|\right]\right\}\mathcal{W}_3\left(x_3,u_3\right)\mathrm{d}x_3.\quad(15)$$

Due to the δ–function in K_{VH}, the integration kernel in eq. (15) depends only on x_3, u_3, and x_4. The kernel indicates the weighting values applied to the input WDF and represents contribution of the input WDF at x_3 and u_3 to Bragg diffraction at x_4. For $x_4=0$, the kernel is plotted in Fig. 3(a). As expected, the spatial frequencies near $u_3=0$ contribute to diffraction significantly in agreement with Bragg theory for this recording geometry. At $x_4=0$, maximum Bragg diffraction is produced by a probe beam with $u_3=0$ and at $x_3=-L\theta_{\mathrm{s}}/2$, instead of $x_3=0$ (see Fig. 3(a) and (b)). The offset is introduced due to the thickness of the VH.

3.B. Spherical wave reference volume hologram (SRVH)

A SRVH is recorded by mutually coherent plane and spherical waves as shown in Fig. 2(b). The refractive index modulation is given by [10]

$$\epsilon(x'', z'') = \exp\left\{-i\frac{\pi}{\lambda}\frac{x''^2}{z'' - z_f}\right\}\exp\left\{i\frac{2\pi}{\lambda}\theta_{\rm s}x''\right\}\exp\left\{-i\frac{\pi}{\lambda}\theta_{\rm s}^2 z''\right\}\mathrm{rect}\left(\frac{z''}{L}\right), \quad (16)$$

where z_f is the distance from the hologram to the point source emitting the spherical wave on the optical axis. The impulse response of the 4–f VH imager is expressed as

$$h(x_2; x_1) = \exp\left\{-i\frac{\pi}{\lambda}\frac{z_f}{f^2}\left(x_1 + x_2 - f\theta_{\rm s}\right)^2\right\}\mathrm{sinc}\left\{\frac{L}{\lambda f^2}\left(x_1 + x_2\right)\left(f\theta_{\rm s} - x_2\right)\right\}. \quad (17)$$

Using the same procedure [12], we obtain the formula for the WDF of the SRVH as

$$\begin{aligned} K_{VH}(x_4, u_4; x_3, u_3) = (\lambda f)^2 \iint \mathrm{d}u_3'\mathrm{d}u_4' \mathrm{e}^{i2\pi\left\{u_4'\left(-\frac{L\lambda}{2}u_4 - x_4\right) - u_3'\left(\frac{L\lambda}{2}u_3 + x_3\right)\right\}} \\ \times \exp\left\{-i2\pi\lambda z_f\left(u_3' + u_4'\right)\left(-u_3 + u_4 - \frac{\theta_{\rm s}}{\lambda}\right)\right\} \\ \times \mathrm{sinc}\left\{L\lambda\left(-u_3 + u_4 + \frac{u_3' + u_4'}{2}\right)\left(u_4 + \frac{u_4'}{2} - \frac{\theta_{\rm s}}{\lambda}\right)\right\} \\ \mathrm{sinc}\left\{L\lambda\left(-u_3 + u_4 - \frac{u_3' + u_4'}{2}\right)\left(u_4 - \frac{u_4'}{2} - \frac{\theta_{\rm s}}{\lambda}\right)\right\}. \quad (18) \end{aligned}$$

The result of numerically integrating $K_{\rm VH}(x_4 = 0, u_4 = \theta_{\rm s}/\lambda; x_3, u_3)$ is shown in Fig. 4(a). As expected, the maximum Bragg diffraction at $x_4 = 0$ and $u_4 = \theta_{\rm s}/\lambda$ is produced by a spherical wavefront (sheared WDF), in which x_3 is not zero due to the finite thickness as shown in Fig 4(b).

4. Conclusion

We presented the formulation for the WDF of VHs with arbitrary refractive index modulation. Since VHs are thick diffractive elements, the conventional approach of computing the WDF for thin transparencies, is not applicable. We proposed a two step procedure: first we compute the impulse response of the 4–f VH imager and then we apply a coordinate transform dictated by the WDF properties to the result of the 4–f VH imager. This end result is the WDF of the VH excluded with the effect of propagation and lenses of the 4–f VH imager. Two common VHs were examined in detail: plane and spherical wave reference VHs, and indicated how Bragg selectivity exhibits itself in Wigner space. *Note that the entire derivation is based on the 1st–order Born approximation, and therefore if the diffraction efficiency is high we may have qualitative differences with respect to more accurate theories, such as coupled wave theory [14]. However, simulation of non-planar wave holograms with coupled–wave theory is not straightforward, whereas our simple theory is more general for volume holograms of small diffraction efficiency.* Potentially the proposed formulation can be applied to other thick optical elements provided that impulse responses are available.

References

1. E. Wigner, "On the quantum correction for thermodynamic equilibrium," Physical Review **40**, 749–759 (1932).

2. M. J. Bastiaans, "Application of the Wigner distribution function in optics," in

"The Wigner Distribution - Theory and Applications in Signal Processing," , W. M. F. Hlawatsch, ed. (Elsevier Science, Amsterdam, 1997), pp. 375–426.

3. K. H. Brenner and J. Ojeda-castañeda, "Ambiguity Function and Wigner Distribution Function Applied to Partially Coherent Imagery," Optica Acta **31**, 213–223 (1984).

4. M. J. Bastiaans, "Wigner Distribution Function and Its Application to 1st-order Optics," Journal of the Optical Society of America **69**, 1710–1716 (1979).

5. M. J. Bastiaans and P. G. J. van de Mortel, "Wigner distribution function of a circular aperture," Journal of the Optical Society of America A **13**, 1698–1703 (1996).

6. V. Arrizón and J. Ojeda-castañeda, "Irradiance at Fresnel Planes of a Phase Grating," Journal of the Optical Society of America A **9**, 1801–1806 (1992).

7. W. Pan, "Double Wigner distribution function of a first-order optical system with a hard-edge aperture," Applied Optics **47**, 45–51 (2008).

8. G. Barbastathis, "The transfer funciton of volume holographic optical systems," in "Photorefractive Materials and Their Applications," , vol. 3 of *Springer Series in Optical Science*, J. P. H. Peter Günter, ed. (Springer-Verlag, 2006).

9. G. Barbastathis and D. Psaltis, "Volume Holographic Multiplexing Methods," in "Holographic Data Storage," , vol. 76 of *Springer Series in Optical Sciences*, H. J. Coufal, D. Psaltis, and G. T. Sincerbox, eds. (Springer, 2000), pp. xxvi, 486, 1st

ed.

10. A. Sinha, W. Sun, T. Shih, and G. Barbastathis, "Volume holographic imaging in transmission geometry," Applied Optics **43**, 1533–1551 (2004).

11. O. Momtahan, C. R. Hsieh, A. Adibi, and D. J. Brady, "Analysis of slitless holographic spectrometers implemented by spherical beam volume holograms," Applied Optics **45**, 2955–2964 (2006).

12. S. B. Oh, "Volume holographic pupils in ray, wave, statistical optics, and wigner space," Ph.D. thesis, Massachusetts Institute of Technology (2009).

13. J. W. Goodman, *Introduction to Fourier optics* (Roberts & Co., Englewood, Colo., 2005), 3rd ed.

14. H. W. Kogelnik, "Coupled wave theory for thick hologram gratings,"Bell System Technical Journal **48**, 2909–2947 (1969).

List of Figures

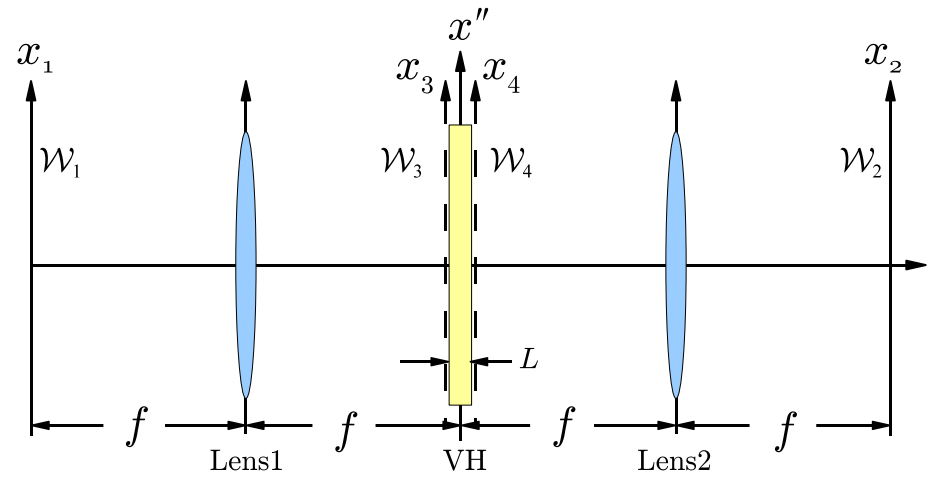

Fig. 1. (Color online) Geometry of the 4–f VH imager, in which a VH is at the Fourier plane of a traditional 4–f telescope.

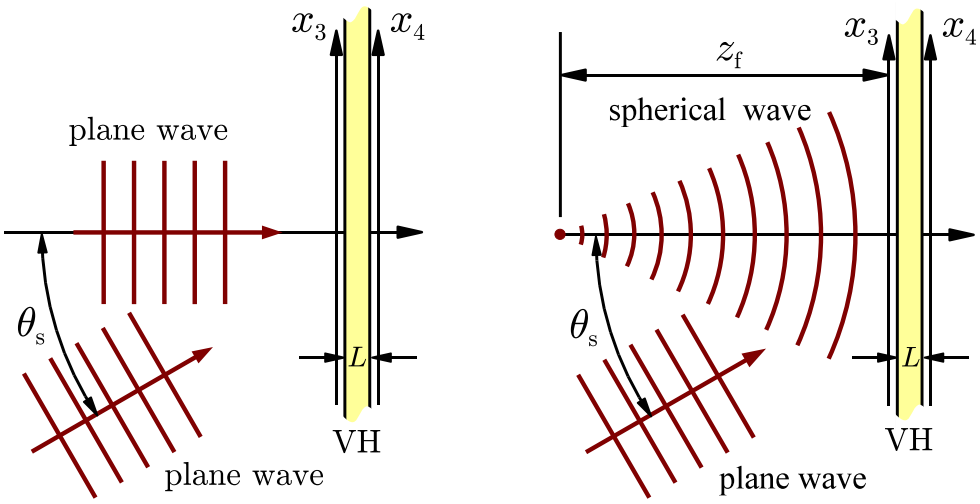

(a) Plane wave reference VH

(b) Spherical wave reference VH

Fig. 2. (Color online) Recording geometries

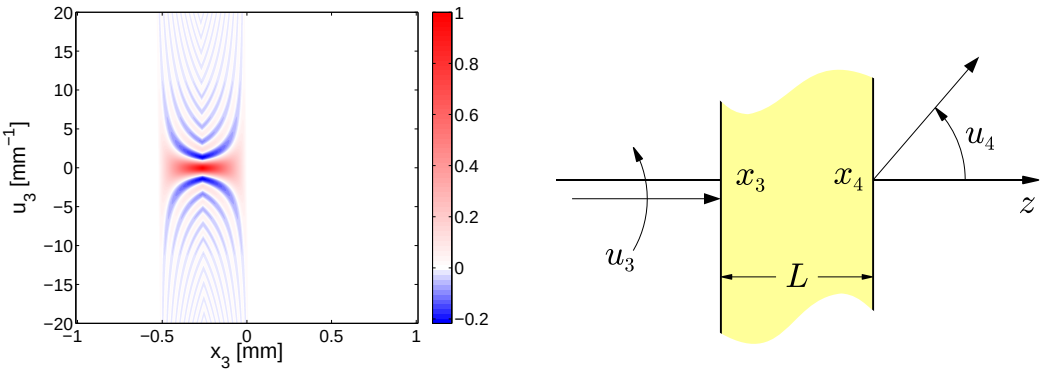

(a) Normalized integration kernel of eq. (15) where $x_4 = 0$.

(b) Geometrical interpretation of (a)

Fig. 3. (Color online) Wigner representation of a PRVH, where $\lambda = 0.5\,\mu$m, $\theta_s = 30°$, and $L = 1$ mm.

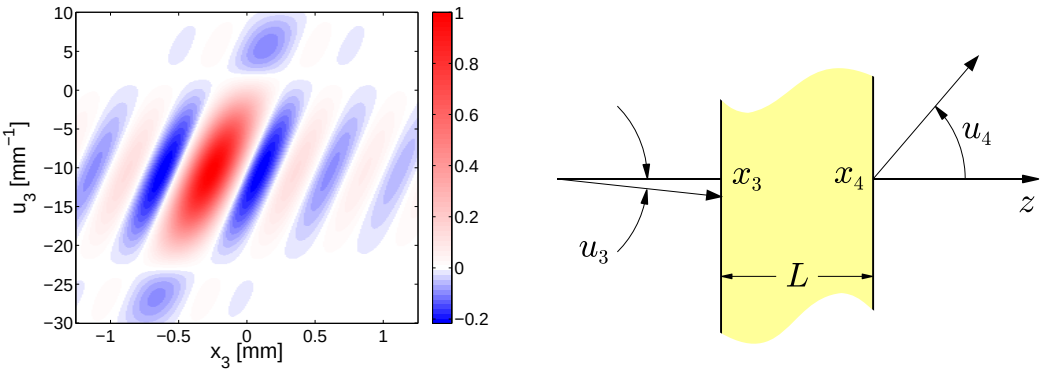

(a) Normalized $K_{\mathrm{VH}}(x_4 = 0, u_4 = \theta_{\mathrm{s}}/\lambda; x_3, u_3)$.

(b) Geometrical interpretation of (a)

Fig. 4. (Color online) Wigner representation of the SRVH, where $\lambda = 0.5\,\mu$m, $\theta_{\mathrm{s}} = 30°$, $z_f = -50\,$mm, and $L = 1\,$mm.